SCIENCE CHINA
Life Sciences

• RESEARCH PAPER •

September 2013 Vol.56 No.9: 811–817
doi: 10.1007/s11427-013-4532-y

Atomic force microscopy imaging of live mammalian cells

LI Mi[1,2], LIU LianQing[1*], XI Ning[3], WANG YueChao[1], DONG ZaiLi[1], XIAO XiuBin[4] & ZHANG WeiJing[4*]

[1]*State Key Laboratory of Robotics, Shenyang Institute of Automation, Chinese Academy of Sciences, Shenyang 110016, China;*
[2]*University of Chinese Academy of Sciences, Beijing 100049, China;*
[3]*Department of Mechanical and Biomedical Engineering, City University of Hong Kong, Hong Kong, China;*
[4]*Department of Lymphoma, Affiliated Hospital of Military Medical Academy of Sciences, Beijing 100071, China*

Received May 28, 2013; accepted July 15, 2013; published online August 7, 2013

Atomic force microscopy (AFM) was used to examine the morphology of live mammalian adherent and suspended cells. Time-lapse AFM was used to record the locomotion dynamics of MCF-7 and Neuro-2a cells. When a MCF-7 cell retracted, many small sawtooth-like filopodia formed and reorganized, and the thickness of cellular lamellipodium increased as the retraction progressed. In elongated Neuro-2a cells, the cytoskeleton reorganized from an irregular to a parallel, linear morphology. Suspended mammalian cells were immobilized by method combining polydimethylsiloxane-fabricated wells with poly-*L*-lysine electrostatic adsorption. In this way, the morphology of a single live lymphoma cell was imaged by AFM. The experimental results can improve our understanding of cell locomotion and may lead to improved immobilization strategies.

atomic force microscopy, cell locomotion, lamellipodia, cytoskeleton, polydimethylsiloxane

Citation: Li M, Liu L Q, Xi N, et al. Atomic force microscopy imaging of live mammalian cells. Sci China Life Sci, 2013, 56: 811−817, doi: 10.1007/s11427-013-4532-y

There are many different types of cells in the human body, each with its own unique size, shape, structure and function. It has been shown that cell shape affects growth, differentiation, development, death and tumor growth [1,2]. Eukaryotic cell shapes, and ultimately the organisms that they form, are defined by cycles of mechanosensing, mechanotransduction and mechanoresponses [3]. Moreover, a cell shape reflects the interactions of many cell components, such as the cytoskeleton, the cell membrane and cell-substrate adhesions [4]. Hence investigating the shape of single cells is of important significance; however, it is difficult to resolve the fine structures of single live cells until the advent of atomic force microscopy (AFM) [5]. AFM uses a sharp tip mounted at the end of a cantilever to raster probe the surface of a sample to construct the topography image of the sample. The main advantages of AFM for characterizing the surface of live cells are that it can be used in liquid environments and that it provides spatial resolution on the nanometer scale [6]. AFM has provided a wealth of novel insights in cell biology, including nanoscale organization and dynamics of cell membranes [7], ultra-structures and activities of organelles [8], and dynamic structures of proteins [9]. AFM has thus become an important tool in cell biology, significantly complementing optical and electron microscopy, and X-ray crystallography.

Until now, most AFM live cell imaging has been focused on adherent mammalian cells and microbial cells. This is because these cells can be readily attached to a flat support. For adherent cells, they can naturally grow and spread on the substrate, therefore we can image them by simply growing them on the substrate [10]. As microbial cells are small and have stiff cell walls, they can be immobilized in

*Corresponding author (email: lqliu@sia.cn; zhangwj3072@163.com)

porous polymer membranes [11] or by poly-*L*-lysine electrostatic adsorption [12]. Suspended mammalian cells, however, are large, soft, and unable to grow on substrates, which prevents these cells from being immobilized like microbial cells. Rosenbluth et al. [13] have used micro-electro-mechanical system (MEMS)-fabricated wells to trap suspended live mammalian cells, but pure mechanical trapping only immobilizes the cells laterally. We developed an immobilization method by combining MEMS pillar mechanical trapping and poly-*L*-lysine electrostatic adsorption [14,15]. This method immobilizes suspended cells in both horizontal (lateral) and vertical (normal) directions and thus enables us to acquire AFM topographies of single living lymphoma cells.

In this paper, we investigated the dynamics of cell locomotion by using time-lapse AFM imaging of adherent mammalian cells. We examined two types of live, adherent mammalian cells (breast cancer cell line MCF-7, neuroblastoma cell line Neuro-2a). Real-time changes of cellular ultra-structures (lamellipodium, cytoskeleton) during cell locomotion were observed by obtaining serial AFM images. For suspended cells, we demonstrated the effectiveness of the presented immobilization method on the B-cell lymphoma cell line (Raji).

1 Materials and methods

1.1 Sample preparation

MCF-7/Raji cells were cultured at 37°C (5% CO_2) in RPMI-1640 containing 10% fetal bovine serum. Neuro-2a cells were cultured at 37°C (5% CO_2) in Dulbecco's modified Eagle's medium containing high glucose and 10% fetal bovine serums. MCF-7/Neuro-2a cells were cultured in Petri dishes and Raji cells were cultured in a flask. The cells were cultured for 24 h before experiments. For MCF-7/Neuro-2a cell imaging, the Petri dishes were taken out of the CO_2 incubator and placed directly on the AFM stage. For Raji cell imaging, polydimethylsiloxane (PDMS)-fabricated well chips were used. The chips were first treated with an oxygen plasma (FEMTO, Diener, Germany), then a poly-*L*-lysine solution was dropped onto the wells and left to dry. Raji cells were harvested by centrifugation at 1000 r min^{-1} for 5 min and then dropped onto the poly-*L*-lysine-coated PDMS well chips. The chips were then attached to a glass slide with a small piece of double-sided adhesive tape and placed into a Petri dish containing phosphate-buffered saline solution (PBS) for AFM imaging.

1.2 PDMS well fabrication

PDMS wells were fabricated using a pillar mold that was produced by MEMS photolithography [14,15]. Liquid PDMS was poured into the pillar mold that was then placed into an 80°C oven for 2 h. After separation from the mold, the solid PDMS had wells that were 10 μm deep and 20 μm in diameter.

1.3 AFM imaging

AFM imaging was performed with a Dimension 3100 AFM (Bruker, Santa Barbara, CA, USA). The MLCT cantilever (Bruker, Santa Barbara, CA, USA) had a normal spring constant of 0.01 N m^{-1} and a tip radius of 20 nm. Under the guidance of AFM's optical microscope, the AFM tip was moved onto the surface of live cells and then the AFM images of the cells were obtained. For adherent mammalian cells (MCF-7/Neuro-2a), the images were acquired in contact mode. To observe the locomotion of the cellular lamellipodium, local areas of the cell were continuously scanned (particularly the cell edges). The interval between each image was 10 min and the entire acquisition time was 2 h. The suspended mammalian cells (Raji) were imaged in tapping mode with a 9.5 kHz drive frequency.

2 Results and discussion

Cell locomotion is of primary importance for embryonic development, wound healing, inflammation, and cancer metastasis [16]. During embryo development, cells migrate to form tissues and organs. Wound healing involves the migration of several cell types, while leukocytes migrate to lymph nodes during inflammation responses [17]. During invasion and metastasis, cancer cells move within tissues [18]. To migrate, a cell must modify its shape and stiffness for interaction with surrounding tissue structures [19]. Cell migration is a coordinated process that involves rapid changes in the dynamics of actin filaments [20], together with the formation and disruption of cell adhesion [21]. In recent years, there have been new insights in terms of calcium flikers [22] and matrix elasticity [23]. However, direct observations of the changes in cellular ultra-structures during cell locomotion have not been widely reported. Here, we demonstrate that time-lapse AFM imaging directly images the dynamics of cell locomotion with nanometer scale resolution.

Figure 1 shows the dynamics of a cellular lamellipodium in the retraction motility of a MCF-7 cell immediately after taking it out of the CO_2 incubator. Figure 1A–L was serial AFM deflection images taken over a 2 h period starting with Figure 1A and ending with Figure 1L. The reference lines in Figure 1A and L clearly show that the cell lamellipodium retracted to the central area of the cell over 2 h. In Figure 1A, the lamellipodium adhered tightly to the substrate and the cytoskeleton was discernible. The lamellipodium began retracting 10 min later and its morphology changed, as shown in Figure 1B. Figure 1C shows how the retraction of the lamellipodium progressed and the cytoskeleton became not visible. After 30 min, four small sawtooth-like filopodia

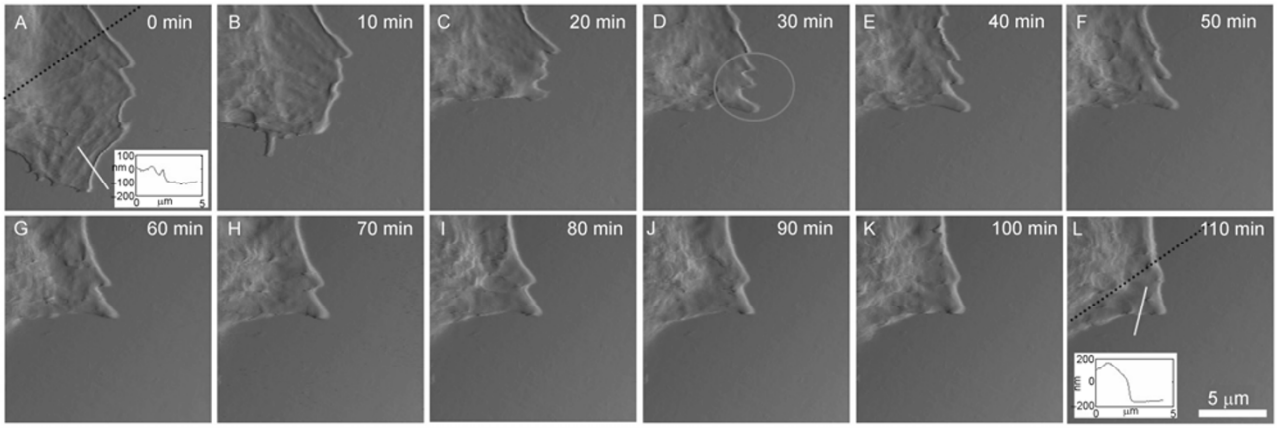

Figure 1 AFM serial images of a MCF-7 cell immediately after leaving the incubator. The cellular lamellipodium retracted toward the cell center and many small filopodium formed (the circle in D). These filopodia eventually reorganized into a new lamellipodium (L). The insets in A and L are the section profiles denoted by the white lines. The dotted line in A and L is the reference line.

formed in the lamellipodium, denoted by the circle in Figure 1D. In Figure 1E, the four filopodia reorganized into three filopodia. In Figure 1F, there were only two filopodia left. From this time on, the speed of changes decreased and finally a new lamellipodium formed (Figure 1L). During the retraction process, the thickness of the lamellipodium was measured by obtaining line profiles of the AFM images (insets in Figure 1A and L). The original thickness of the lamellipodium was about 100 nm (Figure 1A, inset); while the thickness increased significantly to 300 nm after the retraction (Figure 1L, inset).

Figure 2A–L shows serial AFM deflection images of a cellular lamellipodium in another MCF-7 cell taken over a 2 h period. This time, the imaging started 1 h after taking the cell out of the incubator. The dotted line in Figure 2A and L is a reference line. The series of images indicate that the cell did not move and there were no changes of the cellular lamellipodium. The incubator was maintained at 37°C and 5% CO_2, while the environment outside the incubator was at room temperature with atmospheric CO_2 levels. It is possible that an abrupt change in conditions may influence the cell behavior. Thus, we observed the retraction motility of the MCF-7 cell in Figure 1 that was immediately imaged after leaving the incubator. However, 1 h later, the cell may adapt to the environment outside the incubator, and no longer retracts. In fact, we can see that in Figure 1 cell locomotion was not obvious 30 min after the retraction. Generally, cells were still alive 3 h after the AFM experiments [24,25]. Here we performed acquired AFM images within 3 h to insure that the cells were still alive. The exact mechanisms that cause retraction of MCF-7 cells are unknown and further research is needed.

Figure 3 shows the dynamics in the elongation motility of a Neuro-2a cell, obtained 1 h after leaving the CO_2 incubator. Figure 3A–L was AFM deflection images of the axon, where the initial image Figure 3A did not reveal the cytoskeleton. The inset in Figure 3A was the optical image with the axon circled. In contrast to the MCF-7 cell retraction, the locomotion of the Neuro-2a cell was elongation. As the elongation progressed, the cytoskeleton was gradually visualized in the AFM images (Figure 3F–H). The shape of the axon head continuously changed until it became round (Figure 3L). Additionally, the cytoskeleton changed from an irregular (Figure 3I–K) to a linear, parallel ordering, as shown in Figure 3L. Figure 4 shows the dynamics of another Neuro-2a cell, also obtained 1 h after removal from the incubator. The cell did not move, but the cytoskeleton changed in 2 h. As before, the cytoskeleton was not discernible initially (Figure 4A), but was gradually visualized (Figure 4F–L) as it became straightened. From the results of Figures 3 and 4, we can see that the occurrence of the elongation motility phenomenon was cell dependent.

We can see in Figures 1–4 that the behaviors of the MCF-7 cells and Neuro-2a cells differed. We observed the MCF-7 retraction immediately after removing it from the incubator; however, the retraction was not observed 1 h after removing it from the incubator. The Neuro-2a elongation was not universal, but the cytoskeleton changed during each time-lapse AFM image. Time-lapse AFM is a useful tool for characterizing the dynamics of cell activities. Stadler et al. [10] combined AFM with confocal laser scanning microscopy to investigate the dynamics of myoblasts at different stages of myogenesis and directly revealed the membrane structure rearrangements involved in cell division and fusion. Schoenenberger et al. [26] used time-lapse AFM to investigate the cellular dynamics in the locomotion of MDCK cells and revealed changes in cell ultra-structures. Ushiki et al. [27] applied time-lapse AFM to investigate the movements of human esophageal squamous carcinoma cells. Here we used time-lapse AFM to image the dynamics of cell ultra-structures during the locomotion of MCF-7 cells and Neuro-2a cells. The experimental results indicated that the two types of cells have different movements after being taken out of the incubator and that cell locomotion was to

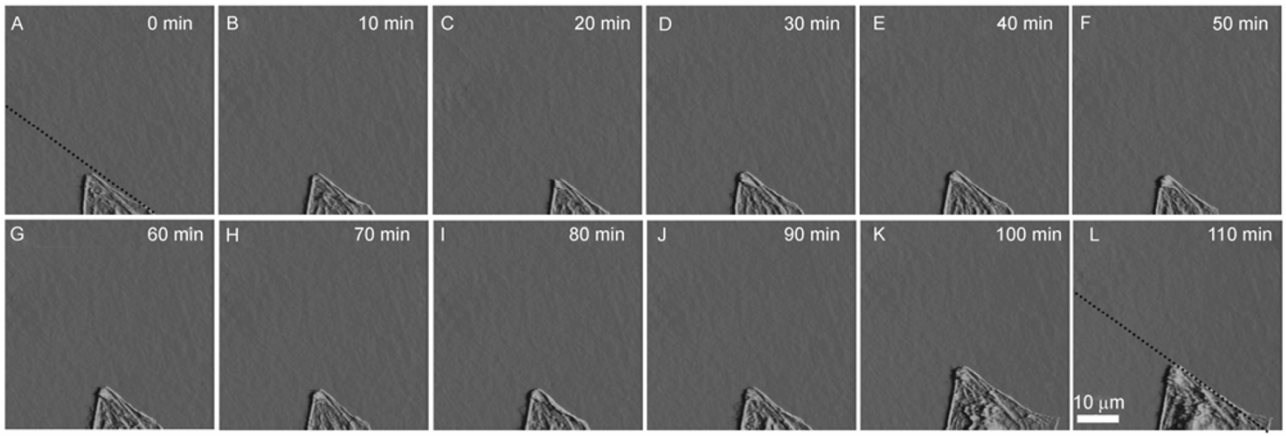

Figure 2 AFM serial images of a MCF-7 cell 1 h after leaving the incubator. The cell did not move. The dotted line in A and L is the reference line.

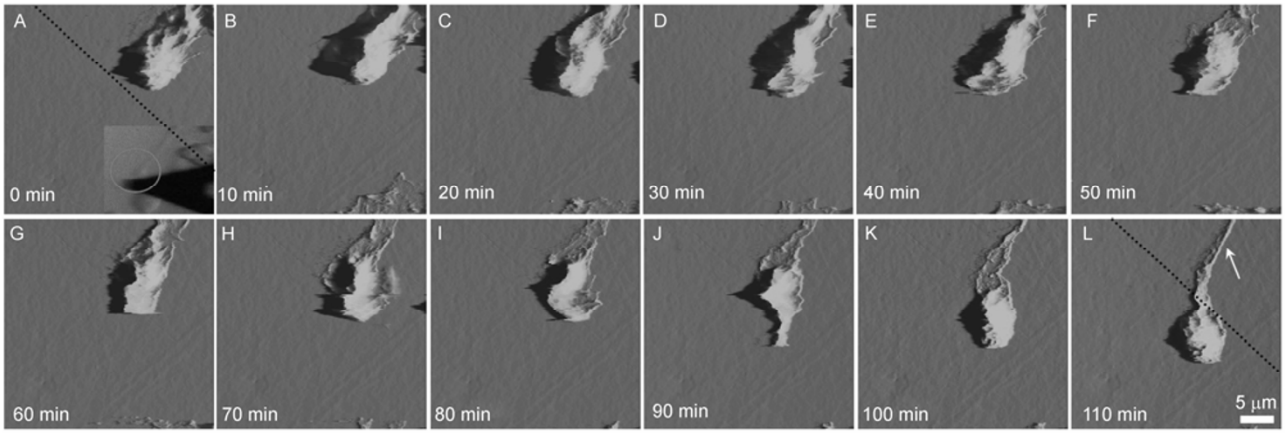

Figure 3 AFM serial images of a Neuro-2a cell 1 h after leaving the incubator. The cellular axon extended on the substrate and the cytoskeleton changed from an irregular organization (I–K) into a parallel, linear one (denoted by the arrow in L). The dotted line in A and L is the reference line. The inset in A is the optical image.

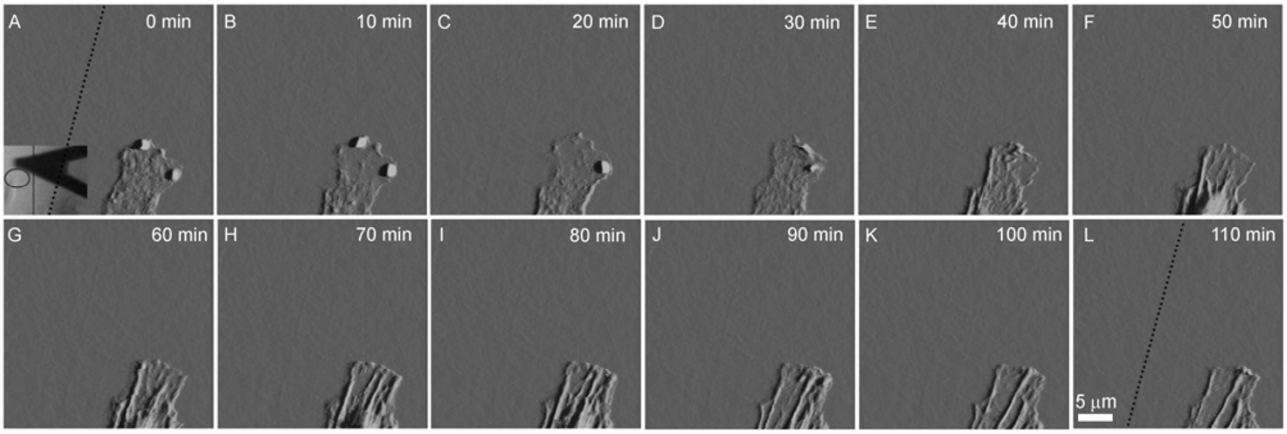

Figure 4 AFM serial images of a Neuro-2a cell 1 h after leaving the incubator. The cytoskeleton changed while the cell did not move. The dotted line in A and L is the reference line. The inset in A is the optical image.

some extent cell-dependent and a function of the time spent out of the incubator.

Suspended mammalian cells can not naturally adhere to the substrate and thus require immobilization. We have previously reported an immobilization technique that combining micro-fabricated pillars with electrostatic adsorption

[14,15]. However, the process of fabricating MEMS pillars is costly and the chips can not be used repeatedly. In contrast, the PDMS chip is inexpensive to fabricate and the mold can be used repeatedly. Figure 5A is a photo of a PDMS-fabricated well chip and Figure 5E is an optical image of the regularly arranged wells. Because PDMS is hydrophobic, the wells should be made hydrophilic. Hydrophobic wells had rounded drops of PBS, as shown in the AFM images in Figure 5B and C. From the line profile (Figure 5D), we can see that the rounded drop exhibited a parabola shape. If the rounded drop was in the well, cells pushed by the AFM probe could not sink into the well. Thus, we used oxygen plasma to clean the chip for 2 min to modify the PDMS surface more hydrophilic and allow cells to settle into the wells. AFM images of the chip after being cleaned by oxygen plasma are shown in Figure 5F and G. From the line profile in Figure 5H we can see that the surface wettability of the PDMS ship was enhanced and the rounded drop vanished.

By combining the PDMS wells with electrostatic adsorption via poly-*L*-lysine, live lymphoma cells were immobilized and AFM images were obtained, as shown in Figure 6. The well can help the cells withstand the lateral scanning force and the poly-*L*-lysine vertically fixes the cells in the well. In the optical image (Figure 6E), the AFM tip was moved onto a cell trapped in a well (denoted by the circle).

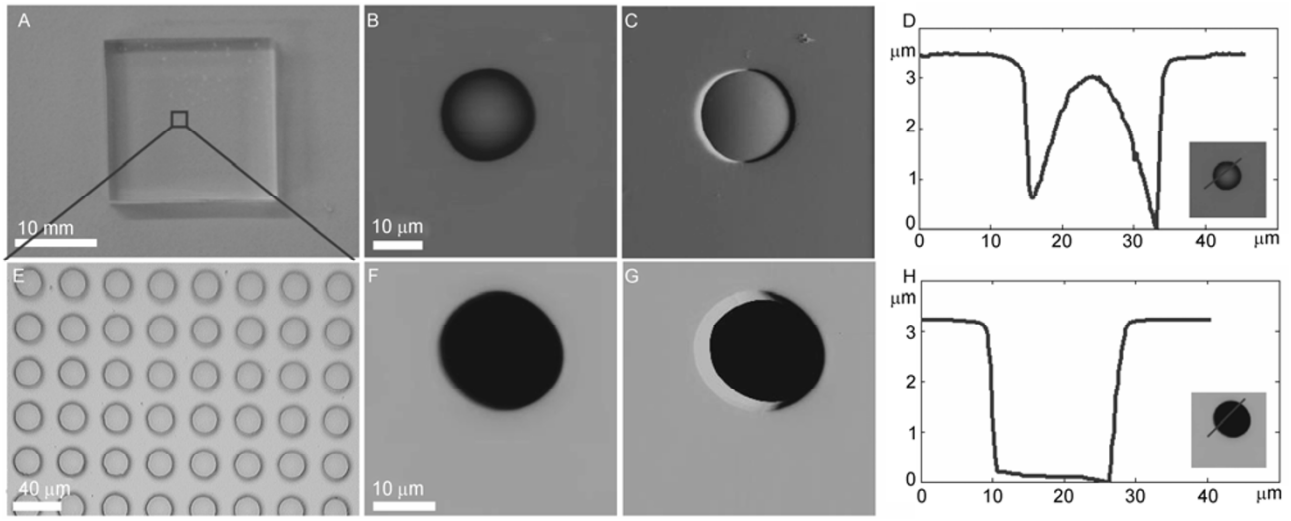

Figure 5 PDMS-fabricated wells. A, PDMS well chip. B and C are AFM images of the PDMS well before plasma cleaning. B, Height image. C, Deflection image. D, Line profile. E, Optical image of the wells. F and G are the AFM images of PDMS wells after plasma cleaning. F, Height image. G, Deflection image. H, Line profile.

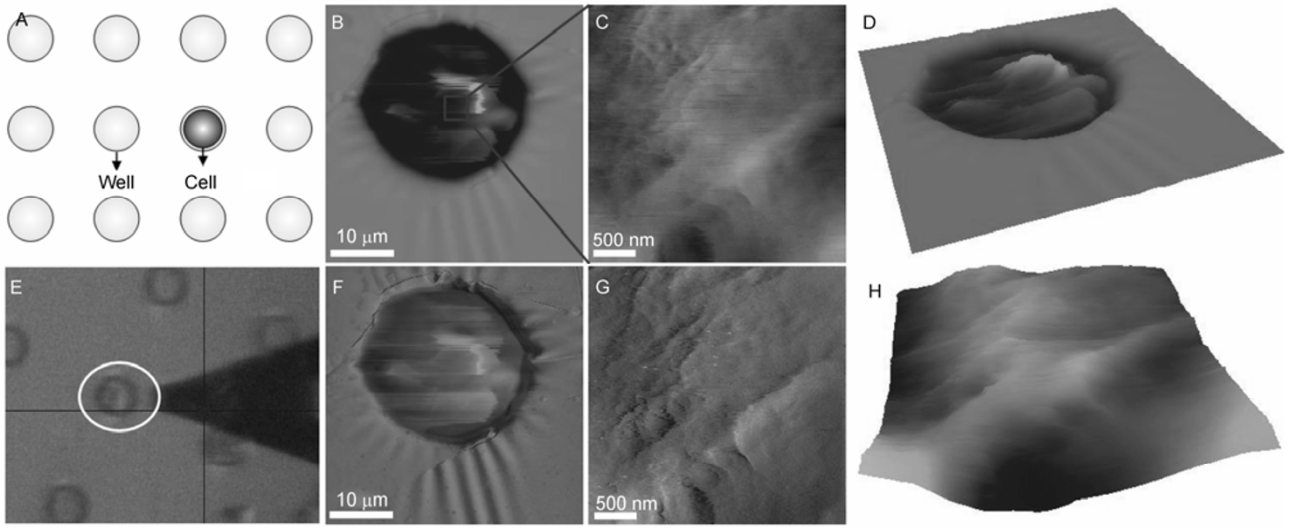

Figure 6 Imaging Raji cells trapped in PDMS wells in PBS. A, Principle of well-based trapping. B, Height images of the whole cell. C, Phase image of the cellular local area. D, Three-dimensional image rendering of height image of the whole cell. E, AFM probe was moved to the trapped cell (denoted by the circle) under the guidance of optical image. F, Phase image of the whole cell. G, Amplitude image of cellular local area. H, Three-dimensional rendering of the amplitude image of the cellular local area.

Figure 6B, D, and F shows the AFM height image, the three-dimensional rendering of the height image, and phase image of the whole cell, respectively. Figure 6C, G, and H shows the AFM phase image, amplitude image and the three-dimensional rendering of the height image of a local area on the cell, respectively. In the local area, the cell exhibited a rough and corrugated morphology. If the well was not coated by poly-*L*-lysine, we found that the cell moved during AFM scanning. Poly-*L*-lysine thus provides an adhesive force between the cell and the bottom of well. The quality of the AFM images of the whole cell are not as good as those obtained when we used micro-fabricated pillars with electrostatic adsorption to immobilize live lymphoma cells [14,15]. This may be because silicon is hydrophilic, while PDMS is hydrophobic. The oxygen plasma treatment may not increase the hydrophilicity of PDMS as much as that for silicon. Furthermore, silicon is stiff, while PDMS is soft, which may also affect the immobilization. The image quality of the reduced area scans (Figure 6C, G, and H) was improved relative to those images of the whole cell (Figure 6B, D, and F). This is because that as the scan size decreased, the influence of cell membrane movement decreased and this cause the image quality increased. Dague et al. [28] used PDMS stamps to trap microbial cells (*Saccharomyces cerevisiae* yeasts and *Aspergillus fumigatus* fungal spores). Microbial cells have thicker, stiffer cell walls, which allow easier acquisition of good quality of AFM images. In contrast, it is a challenge to obtain high quality images of softer, larger mammalian cells because they are easily deformed by the scanning probe [29]. Currently, the resolution of AFM images on live mammalian cells is limited to 50 nm [6]. To increase the AFM resolution, we can try to inhibit the dynamic changes of the cell membrane, such as using films with small pores [30].

3 Conclusion

In summary, AFM is an exciting tool to image and characterize cell surfaces with high resolution [31–34]. Using time-lapse AFM, we directly visualized the real-time changes of cellular ultra-structures (lamellipodium, cytoskeleton) during the locomotion of adherent cells, providing new knowledge about cell locomotion. An immobilization method combining PDMS-fabricated wells and poly-*L*-lysine electrostatic adsorption was presented to trap suspended mammalian cells. In this way, live lymphoma cells were imaged by AFM, facilitating further research on the physiological activities of single live suspended mammalian cells.

This work was supported by the National Natural Science Foundation of China (61175103) and CAS FEA International Partnership Program for Creative Research Teams. We greatly thank Chen Ju, Shang WenYuan, and Professor Ma EnLong from Shenyang Pharmaceutical University for culturing the cells.

1 Mogilner A, Keren K. The shape of motile cells. Curr Biol, 2009, 19: R762–R771
2 Kilian K A, Bugarija B, Lahn B T, et al. Geometric cues for directing the differentiation of mesenchymal stem cells. Proc Natl Acad Sci USA, 2010, 107: 4872–4877
3 Vogel V, Sheetz M. Local force and geometry sensing regulate cell functions. Nat Rev Mol Cell Biol, 2006, 7: 265–275
4 Keren K, Pincus Z, Allen G M, et al. Mechanism of shape determination in motile cells. Nature, 2008, 453: 475–480
5 Binnig G, Quate C F, Gerber C. Atomic force microscope. Phys Rev Lett, 1986, 56: 930–933
6 Muller D J, Dufrene Y F. Atomic force microscopy: a nanoscopic window on the cell surface. Trends Cell Biol, 2011, 21: 461–469
7 Heinisch J J, Lipke P N, Beaussart A, et al. Atomic force microscopy—looking at mechanosensors on the cell surface. J Cell Sci, 2012, 125: 4189–4195
8 Schafer C, Shahin V, Albermann L, et al. Aldosterone signaling pathway across the nuclear envelope. Proc Natl Acad Sci USA, 2002, 99: 7154–7159
9 Mari S A, Pessoa J, Altieri S, et al. Gating of the Mlotik1 potassium channel involves large rearrangements of the cyclic nucleotide-binding domains. Proc Natl Acad Sci USA, 2011, 108: 20802–20807
10 Stadler B, Blattler T M, Franco-Obregon A. Time-lapse imaging of in vitro myogenesis using atomic force microscopy. J Microsc, 2010, 237: 63–69
11 Alsteens D, Dupres V, Yunus S, et al. High-resolution imaging of chemical and biological sites on living cells using peak force tapping atomic force microscopy. Langmuir, 2012, 28: 16738–16744
12 Fatner G E, Barbero R J, Gray D S, et al. Kinetics of antimicrobial peptide activity measured on individual bacterial cells using high-speed atomic force microscopy. Nat Nanotechnol, 2010, 5: 280–285
13 Rosenbluth M J, Lam W A, Fletcher D A. Force microscopy of non-adherent cells: a comparison of leukemia cell deformability. Biophys J, 2006, 90: 2994–3003
14 Li M, Liu L, Xi N, et al. Imaging and measuring the rituximab-induced changes of mechanical properties in B-lymphoma cells using atomic force microscopy. Biochem Biophys Res Commun, 2011, 404: 689–694
15 Li M, Liu L, Xi N, et al. Drug-induced changes of topography and elasticity in living B lymphoma cells based on atomic force microscopy. Acta Phys Chim Sin, 2012, 28: 1502–1508
16 Bershadsky A D, Kozlov M M. Crawling cell locomotion revisited. Proc Natl Acad Sci USA, 2011, 108: 20275–20276
17 Franz C M, Jones G E, Ridley A J. Cell migration in development and disease. Dev Cell, 2002, 2: 153–158
18 Yamazaki D, Kurisu S, Takenawa T. Regulation of cancer cell motility through actin reorganization. Cancer Sci, 2005, 96: 379–386
19 Friedl P, Wolf K. Tumor-cell invasion and migration: diversity and escape mechanisms. Nat Rev Cancer, 2003, 3: 362–374
20 Pollard T D, Cooper J A. Actin, a central player in cell shape and movement. Science, 2009, 326: 1208–1212
21 Mitra S K, Hanson D A, Schlaepfer D D. Focal adhesion kinase: in command and control of cell motility. Nat Rev Mol Cell Biol, 2005, 6: 56–68
22 Wei C, Wang X, Chen M, et al. Calcium flickers steer cell migration. Nature, 2009, 457: 901–905
23 Engler A J, Sen S, Sweeney H L, et al. Matrix elasticity directs stem cell lineage specification. Cell, 2006, 126: 677–689
24 Schaus S S, Henderson E R. Cell viability and probe-cell membrane interactions of XR1 glial cells imaged by atomic force microscopy. Biophys J, 1997, 73: 1205–1214
25 Li Y, Zhang J, Zhang B. Atomic force microscopy study on chlorpromazine-induced morphological changes of living HeLa cells *in vitro*. Scanning, 2009, 31, 259–265

26 Schoenenberger C A, Hoh J H. Slow cellular dynamics in MDCK and R5 cells monitored by time-lapse atomic force microscopy. Biophys J, 1994, 67: 929–936
27 Ushiki T, Hitomi J, Umemoto T, et al. Imaging of living cultured cells of an epithelial nature by atomic force microscopy. Arch Histol Cytol, 1999, 62: 47–55
28 Dague E, Jauvert E, Laplatine L, et al. Assembly of live microorganisms on microstructured PDMS stamps by convective/capillary deposition for AFM bio-experiments. Nanotechnology, 2011, 22: 395102
29 Muller D J, Dufrene Y F. Force nanoscopy of living cells. Curr Biol, 2011, 21: R212–R216
30 Ando T. High-speed atomic force microscopy coming of age. Nanotechnology, 2012, 23: 062001
31 Li M, Liu L Q, Xi N, et al. Detecting CD20-Rituximab interaction forces using AFM single-molecule force spectroscopy. Chin Sci Bull, 2011, 56: 3829–3835
32 Li M, Liu L Q, Xi N, et al. Atomic force microscopy imaging and mechanical properties measurement of red blood cells and aggressive cancer cells. Sci China Life Sci, 2012, 55: 968-973
33 Li M, Liu L Q, Xi N, et al. Progress of AFM single-cell and single-molecule morphology imaging. Chin Sci Bull, doi: 10.1007/s11434-013-5906-z
34 Li M, Liu L Q, Xi N, et al. Mapping CD20 molecules on the lymphoma cell surface using atomic force microscopy. Chin Sci Bull, 2013, 58: 1516–1519